

The effect of the shape of the mesogenic group on the structure and phase behavior of 2,3,4-tris(dodecyloxy)benzenesulfonates with alkaline cations†

 Cite this: *Soft Matter*, 2014, 10, 1746

 Maxim A. Shcherbina,^{*ab} Artem V. Bakirov,^{ac} Andrei N. Yakunin,^d Uwe Beginn,^e Linglong Yan,^f Martin Möller^f and Sergei N. Chvalun^{ac}

Synthesis and mesophase structure characterisation are reported for a group of alkali salts of 2,3,4-tris(dodecyloxy)benzenesulfonic acid. As revealed by a combination of polarizing optical microscopy, differential scanning calorimetry and X-ray scattering, variation of the effective mesogen shape due to changes of the cation size leads to systematic transformation of the materials' phase behaviour. Thermotropic mesophases of different types and dimensionalities were observed: 1D (smectic bilayers), 2D (ordered and disordered columnar phases), and 3D (high-temperature micellar mesomorphic phase, low-temperature crystalline one). Cubic packing prevails when the cation size is small and, thus, the effective mesogen shape is close to the conic one. With increasing ion size, the mesogen shape becomes more tapered, and columnar mesophases appear to be more stable.

 Received 3rd July 2013
 Accepted 2nd December 2013

DOI: 10.1039/c3sm51821c

www.rsc.org/softmatter

Introduction

Supramolecular materials chemistry offers the possibility to generate functional materials containing highly complex structures by exploiting the self-assembling abilities of matter. Instead of forcing the required molecular arrangement and macroscopic morphologies by macroscopic physical experimental techniques ("top down" approach), chemical synthesis is used to design molecular shapes and mutual interactions allowing for the spontaneous formation of the desired structures and functionalities ("bottom up" approach).

Recently a new class of "cunitic"¹ molecules, 2,3,4- and 3,4,5-tris(alkoxy)benzenesulfonates, became of paramount interest for materials design due to a unique richness of their phase behaviour, *i.e.* exhibiting thermotropic and lyotropic smectic, columnar and cubic phases.²⁻⁷ Such compounds are important examples of self-assembling systems which are extremely sensitive to the state of the environment, because even a slight modification of the shape of a molecule, caused by a change in the functional of its free energy,⁸ may significantly alter the shapes of its supramolecular aggregates, which is the reason why the structure of the material can be controlled precisely. For instance, self-assembling under an electric field makes it possible to orient nano-conducting channels on the substrate surface.⁹ Electric fields have also been used to orient structural elements of block-copolymer films.¹⁰ Changes in the structure of supramolecular aggregates containing magnetic nanoparticles and forming photonic crystals were also observed under a magnetic field.¹¹

Benzenesulfonates were also shown to form stable columnar aggregates with temperature-switchable ion channels, organized in a two-dimensional hexagonal lattice stabilized by chemical cross-linking of their aliphatic tails.¹² Such cross-linking was achieved by the introduction of methacryloyl groups near the ends of the aliphatic tails. Subsequent X-ray irradiation leads to the formation of a uniform paraffin matrix with regularly embedded aromatic columns.

Furthermore, these compounds can even form isolated elongated supramolecular structures and organogels from diluted solutions. 2,3,4-Tris(alkoxy)benzenesulfonates are

^aEnikolopov Institute of Synthetic Polymer Materials RAS, 70, Profsoyuznaya street, Moscow, 117393, Russian Federation. E-mail: shcherbina@ispm.ru; Fax: +7 495 7183404; Tel: +7 495 3325815

^bMoscow Institute of Physics and Technology, 9, Institutskiy per., Dolgoprudny, Moscow region, 141700, Russian Federation

^cKurchatov Institute, 1, Kurchatov sq., Moscow, 123098, Russian Federation. E-mail: serge@ispm.ru; Fax: +7 495 7183404; Tel: +7 495 3325815

^dKarpov Institute of Physical Chemistry, 10, Vorontsovo Pole, Moscow, 105064, Russian Federation. E-mail: andreyakunin@yandex.ru; Fax: +7 495 9172490; Tel: +7 495 917430

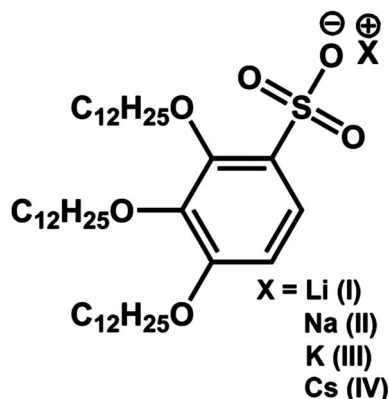
^eUniversität Osnabrück, Institut für Chemie, OMC, BarbarasträÙe 7, D-49076 Osnabrück, Germany. E-mail: ubeginn@uni-osnabrueck.de; Fax: +495419692370; Tel: +495419692790

^fDWI/RWTH Aachen University, Building 5293/DWI Erweiterungsbaus, Forckenbeckstraße 50, 52056 Aachen, Germany. E-mail: moeller@dwi.rwth-aachen.de; Fax: +492418023301; Tel: +492418023300

† Electronic supplementary information (ESI) available. See DOI: 10.1039/c3sm51821c

among the most interesting representatives of cunitic molecules.¹³ They are related in shape to the well-known tris(alkoxy) benzoates,¹⁴ though, being stronger acids, they carry stronger negative charges at the focal point of the mesogenic group.

Moreover, the sulfur atom of the sulfonate tip possesses sp³ hybridization, and, correspondingly, is of spherical shape, while carboxylates contain a flat sp² hybridized carbon centre. For these reasons, 2,3,4-tris(alkoxy)benzenesulfonates allow the study of the effect of charge density as well as the shape of the cunitic tip, or the type, of the used cation on the self-organization, and phase behaviour of the compounds by (i) elucidation of the structure and shape of their respective supramolecular aggregates and (ii) by comparison of such aggregates to those formed by well characterized carboxylate cunitic molecules. These goals will be achieved in the present paper by a comparative analysis of thermotropic liquid crystalline phases formed by four alkali salts of 2,3,4-tris(alkoxy)-benzene-sulfonic acid with substantially different cation sizes, that is lithium- (compound **I**), sodium- (**II**), potassium- (**III**) and caesium- (**IV**) 2,3,4-tris(alkoxy)benzenesulfonate.



As a tentative hypothesis, complex behaviour of the cunitic sulfonate amphiphiles described below may be interpreted in terms of a microphase – segregation model. The large, non-polar alkoxy-benzene-part tends to segregate from the ions, which hence form an ion-cluster phase, confined by the non-polar phase. Since the anion is covalently bound to the non-polar molecule fraction, the two phases cannot move independently. Although it is not required (and, of course improbable) that the cation is permanently fixed in a defined spatial position to a certain sulfonate anion, the macroscopic behaviour is determined by the cation-phase/anion-phase volume ratio. It is hence hypothesized that either Izraelachvili's model of micelle formation¹⁵ or the theories of block-copolymer mesophases^{16,17} may be transferred to the sulfonate amphiphile system. Thus, it may be allowed to discuss the effect of the cation size as if the cation was virtually fixed to the tip of the cunitic anion effective shape approach.

A theoretical approach to an analysis of the effect of the shape of the mesogenic group on materials' phase behaviour was developed by the calculation of the mean radial distribution functions of volume dV/dr for different 3D structures.¹⁸ These functions describe in fact the ideal shape of the dendron that

would form a lattice of particular symmetry. Imagine a sphere of variable radius r with a center coinciding with the centre of each Voronoi polyhedron. Let $v_i(r)$ be the volume of the part of the i^{th} crystalline cell that lies within the sphere. At small r the sphere grows freely; therefore, $dV/dr \sim r^2$. As the sphere approaches the Voronoi polyhedron boundaries, the volume growth rate decreases as the radius increases. To understand the relationship between the calculated volume distributions and the dendron shape, we will consider a conical molecule projected onto a plane which is perpendicular to the cone axis. Then the ideal envelope of this pattern is described by the distribution dV/dr .

This paper also aims to extend an analysis of the self-assembly of tapered and conical dendrons on a new class of cunitic molecules: 2,3,4-tris(alkoxy)benzenesulfonate derivatives.

Experimental methods

X-ray scattering

The structures of the compounds **I–IV** were investigated by means of small- and wide-angle X-ray diffraction methods. High resolution 2-D SAXS patterns have been obtained, using a *NanoStar Bruker*® AXS diffractometer (CuK α -radiation, $\lambda = 1.5406 \text{ \AA}$) with a proportional *Hi-Star* detector and point collimation systems on the basis of Göbel mirror (forming slit diameters are 0.75, 0.4 and 1.0 mm respectively). The device setup allowed us to record scattering patterns in the range of wave vector amplitudes, corresponding to d -spacings from 0.8 nm to 17.5 nm. The exposure time varied from 400 to 2000 s, depending on the intensity of scattered radiation.

X-Ray diffraction patterns in small and wide angle scattering regions were also recorded using an *S3-Micropix* system (*Hecus* company), CuK α -radiation, $\lambda = 1.5406 \text{ \AA}$ with a *Xenocs Genix* source (voltage and current are 50 kV and 1 mA respectively). A *Pilatus 100K* detector was employed, as well as a linear *PSD 50M* gas detector (Ar–Me mixture at $8 \times 10^5 \text{ Pa}$). The collimation system *Fox 3D* with Kratky collimation slits of 0.1 mm and 0.2 mm width was used, allowing reliable measurements in a wave vector range from $q = 0.003 \text{ \AA}^{-1}$ to $q = 1.9 \text{ \AA}^{-1}$ where $q = 4\pi \sin \theta/\lambda$ and 2θ is the scattering angle. To get rid of the scattering of X-rays on air molecules, Göbel mirrors and scattering path had been vacuumed (residual air pressure is about $2.6 \div 5.0 \text{ Pa}$). The exposure time varied from 600 to 5000 s. The thermal behavior of samples was studied using Joule attachment in the temperature range from $23 \text{ }^\circ\text{C}$ to $300 \text{ }^\circ\text{C}$.

Nascent powder samples were put between two ultrathin polyimide films and installed into the holder of the vacuumed X-ray camera. This design was chosen to ensure that the samples remained in vacuum in the course of the X-ray experiment.

Domain sizes L and paracrystallinity parameter g were estimated, using the Hoseman–Bonart method¹⁹ from integral half-widths Δs of several (usually two) reflection orders:

$$\frac{1}{L_n^2} = \left(\frac{\Delta q}{2\pi}\right)^2 - \left(\frac{\pi g^2 n^2 q_{hik}^{(n)}}{2}\right)^2 \quad (1)$$

Electron density maps

Electron density maps were calculated, using structural factors F_{hkl} , obtained from experimental intensities of X-ray reflection maxima $I(s_{hkl})$:

$$I(s_{hkl}) \propto F_{hkl}^2 mLP \quad (2)$$

Corrections on reflection repetition m and Lorentz factor $L \sim q_{hkl}^{-2}$ (ref. 20) have been made. Polarization factor P equals to unity for the geometrical setups used.

According to the general theory of diffraction,²⁰ periodic functions of electron density $\rho(r)$ can be represented as Fourier series whose coefficients are structural factors of individual reflections F_{hkl} :

$$\Delta\rho \equiv \rho(r) - \rho_0 \propto \sum_{hkl} F_{hkl} \exp[-2\pi i(hx + ky + lz)] \quad (3)$$

where ρ_0 is an average electron density and x, y, z are partial coordinates of unit cell nodes. Phase coefficients of every term in this sum are imaginary numbers, thus a reconstruction of electron density is impossible for arbitrary crystal cells. However, there exist several important cases, in which the imaginary part of every term in eqn (3) is equal to zero. For such symmetries, a choice of the phase factor for every reflection is reduced to a choice of its sign: “+” for a phase of (hkl) which is equal to zero, and “-” for a phase angle of π . For instance, in cubic centrosymmetric crystal lattices:²¹

$$\Delta\rho \propto \sum_{hkl} \pm |F_{hkl}| \cos[2\pi(hx + ky + lz)] \quad (4)$$

Another important case of such possibilities is cylinder symmetry of the system. The electron density distribution can here be rewritten in cylindrical coordinates as:

$$\rho(r, \psi, z) = \int_0^\infty \int_0^{2\pi} \int_0^\infty F(R, \psi, Z) \times \exp[-2\pi(Rr \cos(\psi - \Psi) + Zz)] R dR d\Psi dZ \quad (5)$$

Taking into account cylindrical symmetry of the system, one can rewrite eqn (5), as:

$$\rho(r) = 2\pi \sum_i \pm |F(R_i)| J_0(2\pi R_i r) R_i \Delta R_i \quad (6)$$

where J_0 represents the Bessel function of 0th order, i is the sequence number of the reflection, and ΔR_i is its integral half-width.

For f reflections experimentally observed, there are 2^f permutations of phase signs. Accurate determination of phase signs is a particular important structural problem. Its unambiguous solution requires the use of a number of additional approaches and techniques. The most widely used criterion for the choice of phase signs is that their correct combination causes a minimum value of the fourth moment of electron density fluctuations $\langle(\Delta\rho)^4\rangle$:²²

$$\langle(\Delta\rho(r))^4\rangle \propto \frac{1}{V} \int (\Delta\rho(r))^4 dV \quad (7)$$

where V is the unit cell volume, and

$$\Delta\rho(r) = \frac{\rho(r) - \langle\rho\rangle}{\sqrt{\rho^2(r) - \langle\rho\rangle^2}} \quad (8)$$

is the dimensionless normalized density fluctuation (map of electron density distribution).

Another approach to the choice of correct phase combination includes the construction of electron density histograms, and their comparison with theoretical ones. An application of this technique to the structural studies of cubic mesophases formed by dendrons on the basis of gallic acid can be found in ref. 22. It should be noted also that electron density reconstruction appears to be a quite reliable technique, when more than three or four X-ray reflections are used. Hence, it is very important to compare the electron density maps obtained with the results of molecular modelling, showing the principal possibility of one or another packing of the matter into supramolecular aggregates of known macroscopic density and shape.

Thermal analysis

Thermal analysis was carried out, using a “Perkin Elmer DSC-7” calorimeter, heating-cooling rates being 10 and 20 °C min⁻¹, respectively. Phase transition temperatures were defined as the maxima of the corresponding endo- and exo-thermal peaks appearing in the thermograms.

NMR-spectroscopy

¹H-NMR (300 MHz) and ¹³C-NMR (75 MHz) spectra were recorded on a Bruker DPX-300 spectrometer with tetramethylsilane (TMS) as an internal standard in deuterated chloroform at 20 °C.

Elemental analysis

The carbon and hydrogen elemental composition was determined in the Microanalytical Laboratory Kolbe, Mühlhausen, Germany.

Molecular modeling

The *Accelrys Materials Studio* program set was employed for molecular modelling of compounds studied. We used two sets of potentials which allow us to take into account the non-covalent interactions of the mesogenic groups inside the cylinders of the columnar mesophases: COMPASS (Condensed-phase Optimized Molecular Potentials for Atomistic Simulation Studies) and UFF (Universal Force Field). The COMPASS set is suitable for modelling of isolated molecules and condensed phases of mainly organic, polymeric and of some inorganic compounds,^{23–25} it also allows us to parameterise partial charges and valences *ab initio* with subsequent system optimization. To prove the results of modelling, we applied UFF potentials, used for calculation of geometry of organic molecules containing metal-organic complexes. UFF does not have any limitation on the chemistry of compounds involved.^{26–28}

Synthesis

Synthesis of the studied compounds is described in detail elsewhere.¹ ¹H and ¹³C NMR spectra of compounds I–IV can be found in the ESI.†

Materials

1,2,3-Trihydroxy-benzene (99+%, Aldrich), 1-bromododecane (99+%, Aldrich), potassium carbonate (97%, Aldrich), sulfuric acid (95–97%, Merck), methyllithium (Aldrich), sodium methanolate (ACS reagent), potassium methanolate (ACS reagent), caesium hydroxide (97%, Aldrich), and potassium carbonate (ACS reagent) were used as received. Ethanol, methanol, acetone, diethylether, *n*-hexane, toluene, ethyl acetate, tetrahydrofuran, dichloromethane, isopropyl ether, and all ACS reagents were used as received. DMF (ACS reagent grade) was dried over calcium hydride (CaH₂) for 12 h and distilled in a vacuum. All deuterated solvents for NMR studies were received from Chemotrade (Leipzig).

1,2,3-Tris(dodecyloxy)benzene (1). 10.1 g (0.08 mol) 1,2,3-trihydroxy-benzene and 55.5 g (0.4 mol) K₂CO₃ were mixed with 125 ml of freshly dried DMF in a 250 ml three-necked flask with a magnetic stirrer under a nitrogen atmosphere. At 60 °C, 55.2 ml (0.23 mol) 1-bromododecane was added dropwise. The reaction mixture was stirred for 5 hours at 60 °C. After reaction, the mixture was slowly poured into 600 ml ice water. The precipitate was isolated by filtration and then dried *in vacuo*. The crude product was recrystallized from 300 ml acetone three times to yield a white powder. Yield: 38.3 g (76% of theory); m.p. 39–40 °C; TLC (*n*-hexane–EtOAc = 20 : 1): *R*_f = 0.68; ¹H NMR (300 MHz, CDCl₃, 20 °C, TMS, δ, ppm): 0.88 (t, 9H, CH₃, *J* = 6.6 Hz), 1.26 (overlapped peaks, 48H, CH₃(CH₂)₈), 1.47 (m, 6H, O(CH₂)₂CH₂), 1.78 (m, 6H, O(CH₂)CH₂), 3.90 (overlapped t, 6H, OCH₂, *J* = 6.3 Hz), 6.55 (d, 2H, 4,6-benzene-H, *J* = 8.1 Hz), 6.90 (t, 1H, 5-benzene-H, *J* = 8.4 Hz); ¹³C NMR (75 MHz, CDCl₃, 20 °C, TMS, δ, ppm): 14.1 (CH₃), 22.7 (CH₃CH₂), 26.1 (OCH₂CH₂CH₂), 29.4 (CH₃CH₂CH₂CH₂), 29.5 (CH₃CH₂CH₂CH₂(CH₂)₅), 29.9 (1,3-OCH₂CH₂), 30.3 (2-OCH₂CH₂), 31.9 (CH₃CH₂CH₂), 69.0 (1,3-OCH₂), 73.3 (2-OCH₂O), 106.7 (4,6-benzene-C), 123.1 (5-benzene-C), 138.4 (2-benzene-C), 153.4 (1,3-benzene-C).

2,3,4-Tris(dodecyloxy)benzenesulfonic acid (2). Under a nitrogen atmosphere, 1.27 g of **1** (2.0 mmol) was added into 10 ml of concentrated sulfuric acid (95–97%) at 0 °C. The reaction suspension was stirred for 2 hours while the temperature of the water was gradually increased until 20 °C. The suspension was poured slowly into 50 ml of ice water. The resulting light-yellow suspension was kept at 4 °C for 1 hour and the precipitate was isolated by filtration and pre-dried *in vacuo*. The crude product was recrystallized from 30 ml acetone at 4 °C three times and dried *in vacuo* to yield a white powder. Yield: 1.24 g (87.2% of theory); m.p. 65.0–65.5 °C; ¹H NMR (300 MHz, CDCl₃, 20 °C, TMS, δ, ppm): 0.88 (t, 9H, CH₃, *J* = 6.7 Hz), 1.27 (overlapped peaks, 48H, CH₃(CH₂)₈), 1.45 (m, 6H, O(CH₂)₂CH₂), 1.83 (m, 6H, O(CH₂)CH₂), 4.00 (overlapped t, 4H, 3- and 4-OCH₂), 4.29 (t, 2H, 2-OCH₂, *J* = 6.98 Hz), 6.69 (d, 1H, 5-benzene-H, *J* = 9.06 Hz), 7.54 (d, 1H, 6-benzene-H, *J* = 8.85 Hz); ¹³C NMR (75 MHz, CDCl₃, 20 °C, TMS, δ, ppm): 14.13, 22.70, 25.77, 26.10, 29.11,

29.39, 29.72, 30.00, 30.29, 31.94, 73.96, 75.77, 107.40, 123.20, 124.78, 141.89, 149.73, 157.79; IR (KBr, cm⁻¹): 3435.11 (s, broad), 2956.86 (m), 2917.63 (vs), 2851.29 (s), 1732.56 (w), 1631.30 (w), 1582.85 (w), 1486.22 (w), 1466.57 (m), 1441.26 (w), 1380.14 (w), 1304.58 (w), 1281.34 (w), 1226.56 (m), 1162.99 (w), 1087.42 (s), 1041.04 (w), 885.31 (w), 802.42 (w), 787.36 (w), 719.54 (w), 709.03 (w), 691.90 (w), 634.69 (w), 606.35 (w), 578.87 (w), 531.66 (w); elemental analysis calculated (%): C 71.04, H 10.93; found (%): C 69.13, H 11.32.

Lithium 2,3,4-tris(dodecyloxy)benzenesulfonate (I). In a nitrogen atmosphere, 0.2 ml (0.32 mmol) ether solution of methyl lithium (1.6 mol L⁻¹) was added into 5 ml of freshly dried ether solution of compound **2** (227.6 mg, 0.32 mmol) at room temperature. The reaction mixture was stirred for 2 hours, subsequently the solvent was removed under vacuum using a membrane pump. The solid obtained was dried at 40 °C in an oil-pump vacuum to yield a white powder of **I**. Yield: 0.2 g (≈ 87% of theory); m.p. –11.1 °C (by DSC); TLC (EtOAc–MeOH = 6 : 1): *R*_f = 0.45; ¹H NMR (300 MHz, CDCl₃, 20 °C, TMS, δ, ppm) (Fig. S1 of ESI†): 0.88 (t, 9H, CH₃, *J* = 6.23 Hz), 1.26 (overlapped peaks, 54H, CH₃(CH₂)₉), 1.77 (m, 6H, O(CH₂)CH₂), 3.84 (broad, 4H, 3- and 4-OCH₂), 4.08 (broad, 2H, 2-OCH₂), 6.34 (broad, 1H, 5-benzene-H), 7.34 (d, 1H, 6-benzene-H, *J* = 8.28 Hz); ¹³C NMR (75 MHz, CDCl₃, 20 °C, TMS, δ, ppm) (Fig. S2 of ESI†): 14.12, 22.72, 25.75, 26.33, 29.44, 29.55, 29.81, 30.53, 31.99, 32.04, 68.62, 73.67, 106.85, 123.74, 128.96, 141.82, 150.02, 155.73; elemental analysis calculated (%): C 70.35, H 10.85; found (%): C 68.28, H 10.97.

Sodium 2,3,4-tris(dodecyloxy)benzenesulfonate (II). In a nitrogen atmosphere, 19.0 mg (0.35 mmol) sodium methoxide was dissolved in 5 ml of freshly dried methanol. Subsequently, 250 mg (0.35 mmol) of compound **2** was added, and the reaction mixture was stirred vigorously for 2 hours at room temperature. Afterwards, the solvent was removed under vacuum using a membrane pump. The solid obtained was freeze-dried from benzene *in vacuo* to yield a white powder of **II**. Yield: 0.21 g (82% of theory); m.p. 7.7 °C (by DSC); TLC (EtOAc–MeOH = 6 : 1): *R*_f = 0.34; ¹H NMR (300 MHz, CDCl₃, 20 °C, TMS, δ, ppm) (Fig. S4 of ESI†): 0.88 (overlapped t, 9H, CH₃), 1.26 (overlapped peaks, 54H, CH₃(CH₂)₉), 1.67 (broad, 6H, O(CH₂)₂CH₂), 3.79 (broad, 4H, 2,4-OCH₂), 4.03 (broad, 2H, 3-OCH₂), 6.18 (broad, 1H, 5-benzene-H), 7.28 (broad, 1H, 6-benzene-H); ¹³C NMR (75 MHz, CDCl₃, 20 °C, TMS, δ, ppm) (Fig. S5 of ESI†): 14.12, 22.74, 25.74, 26.42, 29.51, 29.60, 29.70, 29.95, 30.63, 32.01, 68.54, 73.47, 75.42, 106.61, 123.85, 128.90, 141.77, 150.20, 155.30; elemental analysis calculated (%): C 68.61, H 10.59; found (%): C 67.32, H 11.16.

Potassium 2,3,4-tris(dodecyloxy)benzenesulfonate (III). In a nitrogen atmosphere, 61.6 mg (0.88 mmol) potassium methoxide was dissolved in 10 ml of freshly dried methanol. Subsequently, 625.4 mg (0.88 mmol) of compound **2** was added, and the reaction mixture was stirred vigorously for 2 hours at room temperature. Finally, the solvent was removed under vacuum using a membrane pump. The solid obtained was freeze-dried from benzene *in vacuo* to yield a white powder of **III**. Yield: 0.62 g (94% of theory); m.p. 17.8 °C (by DSC); TLC (EtOAc–MeOH = 6 : 1): *R*_f = 0.16; ¹H NMR (300 MHz, CDCl₃, 20

°C, TMS, δ , ppm) (Fig. S6 of ESI†): 0.88 (overlapped t, 9H, CH₃), 1.26 (overlapped peaks, 54H, CH₃(CH₂)₉), 1.75 (m, 6H, OCH₂CH₂), 3.84 (broad, 4H, 3- and 4-OCH₂), 4.07 (broad, 2H, 2-OCH₂), 6.29 (d, 1H, 5-benzene-H, $J = 8.28$ Hz), 7.35 (d, 1H, 6-benzene-H, $J = 8.70$ Hz); ¹³C NMR (75 MHz, CDCl₃, 20 °C, TMS, δ , ppm) (Fig. S7 of ESI†): 14.12, 22.73, 25.83, 26.39, 29.49, 29.58, 29.92, 30.62, 32.03, 68.56, 73.55, 74.96, 106.79, 123.63, 130.71, 142.00, 150.34, 155.23; elemental analysis calculated (%): C 67.33, H 10.36; found (%): C 66.36, H 10.49.

Caesium 2,3,4-tris(dodecyloxy)benzenesulfonate (IV). In a 100 ml two-necked flask with a magnetic stirrer in a nitrogen atmosphere, 0.71 g (1.00 mmol) of **2** was dissolved in 50 ml methanol at 60 °C. Subsequently, 0.34 g (2.0 mmol) of caesium hydroxide was added. The reaction mixture was refluxed for 30 minutes, and was filtered hot. The filtrate was cooled to room temperature, the precipitate was isolated by filtration and washed with water until the washing water became neutral. After pre-drying *in vacuo*, the crude product was twice crystallized from *n*-hexane to obtain a white powder of **IV**. Yield: 0.8 g (98% of theory); m.p. 50.3 °C (by DSC); TLC (CHCl₃-MeOH = 6 : 1): $R_f = 0.44$; ¹H NMR (300 MHz, CDCl₃, 20 °C, TMS, δ , ppm) (Fig. S8 of ESI†): 0.88 (t, 9H, CH₃, $J = 6.6$ Hz), 1.26 (overlapped peaks, 48H, CH₃(CH₂)₈), 1.47 (broad, 6H, O(CH₂)₂CH₂), 1.72 (m, 6H, OCH₂CH₂), 3.90 (overlapped peaks, 6H, OCH₂, $J = 6.6$ Hz), 7.03 (s, 2H, 2,6-position); ¹³C NMR (75 MHz, CDCl₃, 20 °C, TMS, δ , ppm) (Fig. S9 of ESI†): 14.12, 22.71, 26.27, 29.44, 29.62, 29.80, 31.96, 73.42, 106.7, 139.52, 140.03, 152.99; elemental analysis calculated (%): C 59.84, H 9.21; found (%): C 59.71, H 9.23.

Results and discussion

Structure and phase behaviour of lithium 2,3,4-tris(dodecyloxy)benzenesulfonate

The lithium cation is the smallest amongst the alkali metals, and the shape of an isolated lithium 2,3,4-tris(dodecyloxy)benzenesulfonate (**I**) molecule can be reliably described as a sharp V-cone. As revealed by differential scanning calorimetry (Fig. 1), three subsequent phase transitions of compound **I** take place upon its heating at 93 °C, 118 °C and 161 °C ($\Delta H_1 = 48.1$ kJ mol⁻¹; $\Delta H_2 = 4.7$ kJ mol⁻¹ and $\Delta H_3 = 0.27$ kJ mol⁻¹ respectively). The latter one corresponds to the material isotropization, and the second signal is accompanied by the simultaneous loss of birefringence, corresponding to the transition into an optically isotropic phase.

X-Ray diffractograms of the “as-received” compound **I** are characterized by two sets of reflections, consisting of three peaks with d -spacing ratio 1 : 2 : 3 (Fig. 2, curve 1, see ESI, Table S1†). They correspond to interlayer distances of $L_1 = 3.64$ nm and $L_2 = 3.27$ nm respectively. Separate analysis of the phase behaviour of materials either in the vacuum of the X-ray camera or in an especially designed air-conditioned holder allowed us to explain unequivocally this pattern by the presence of two different layered structures, the latter one ($L_2 = 3.27$ nm) formed in the presence of water molecules by self-assembly of benzenesulfonate derivatives’ hydrates, and the former one organized by benzenesulfonate dendrons only. The analysis of wide-angle X-ray patterns revealed that the as-received phase is

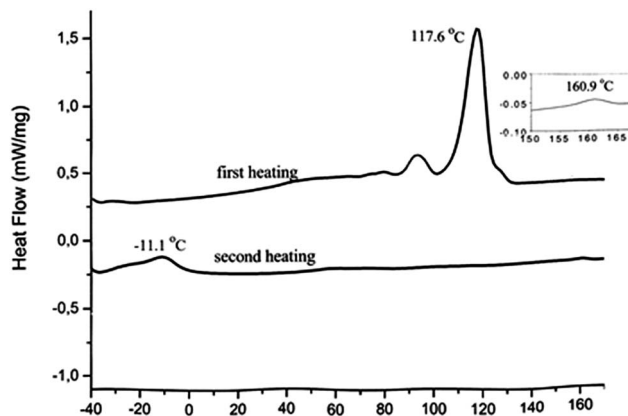


Fig. 1 DSC scans of lithium 2,3,4-tris(dodecyloxy)benzenesulfonate. The inset shows high-temperature low-heat transformation on first heating.

a crystalline one. The proposed structure, then, could be described either by two coexistent crystalline layer-type mesophases or by the formation of a complex smectic mesophase in which ordered layers of in-plane benzenesulfonate dendrons are separated by water. With increasing temperature water evaporates leading to the drop in smectic interlayer distance with a subsequent reorganization of the benzenesulfonic groups which manifests itself in a drastic change of the wide-angle scattering patterns as well (inset in Fig. 2).

It should be noted, however, that nascent crystalline phases formed by the “as-received” samples undergo irreversible transitions and thus can be ascribed to the effect of solvents or hydrate complexes formed during the synthesis of the

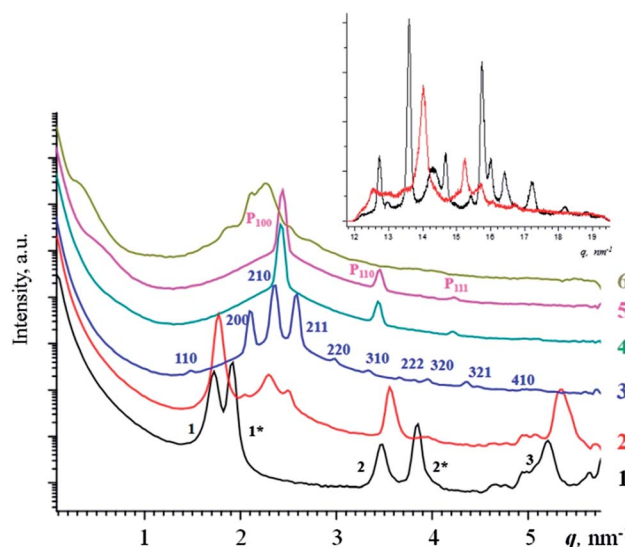


Fig. 2 Small-angle scattering for lithium 2,3,4-tris(dodecyloxy) benzenesulfonate at 20 °C (1), 95 °C (2), 130 °C (3), 170 °C (4), 220 °C (5) and 200 °C cooling (6); one-digit indices show the reflections of layer structures, three-digit ones correspond to a high-temperature cubic mesophase of $Pm\bar{3}n$ symmetry. The inset shows WAXS patterns of the material at 20 °C (black) and 90 °C (red).

compounds. Such “virgin phases” hence do not play a significant role in the studies of the materials phase behaviour.

Heating the samples up to 95 °C is accompanied by a decrease of the interlayer distances with thermal expansion coefficients $\beta_1 = -2.2 \times 10^{-4} \text{ K}^{-1}$ and $\beta_2 = -2 \times 10^{-4} \text{ K}^{-1}$ down to $L_1 = 3.58 \text{ nm}$ and $L_2 = 3.22 \text{ nm}$ respectively (see ESI, Table S2†).

This effect is rather common for liquid crystalline materials, and can be explained by effective shrinking of aliphatic tails with increasing temperature due to the accumulation of gauche-conformers.

According to molecular modelling, the length of the lithium 2,3,4-tris(dodecyloxy) benzene-sulfonate ion-pair is 2.25 nm if alkyl tails are fully extended. This is substantially smaller than the interlayer distance, thus it was concluded that the observed smectic layers have a bilayer structure (cf. Fig. 3). The difference between the observed interlayer distance and the doubled molecule length ($\Delta l = 0.9 \text{ nm}$) can be attributed to a partial inter-penetration of alkyl tails of opposing molecules. It should be noted that in the temperature interval of the first transition ($\sim 95 \text{ °C}$) reflections of the crystal-hydrate structure lose their intensity abruptly revealing the order–disorder transition in the layer structure due to the loss of water molecules which has been confirmed by the results of thermogravimetric analysis (see ESI, Fig. S3 and S10†).

Moreover, a new set of four reflections appears, yielding a d -spacing square ratio of $d_{200}^2 : d_{210}^2 : d_{211}^2 : d_{310}^2 = 4 : 5 : 6 : 10$, which is highly specific for the cubic phase of $Pm\bar{3}n$ symmetry ($a = 5.95 \text{ nm}$), see ESI, Table S3.† On further heating to 130 °C the transition into the cubic mesophase has become fully developed, one can observe at least eleven reflections (Fig. 2, curve 3) indexed by the $Pm\bar{3}n$ symmetry unit cell. Thus, the loss of optical birefringence can unambiguously be related to the transition from a smectic bilayer structure, formed during the synthesis of the compounds with participation of some crystal-hydrates and subsequent drying, into a cubic mesophase. Such a transition is probably due to the change of the volume fractions of the aliphatic chains within the mesogenic groups, which, in turn, defines an equilibrium interphase curvature.^{29,30} It should also be noted that an increasing mobility of alkyl tails leads to the change of the general molecular shape

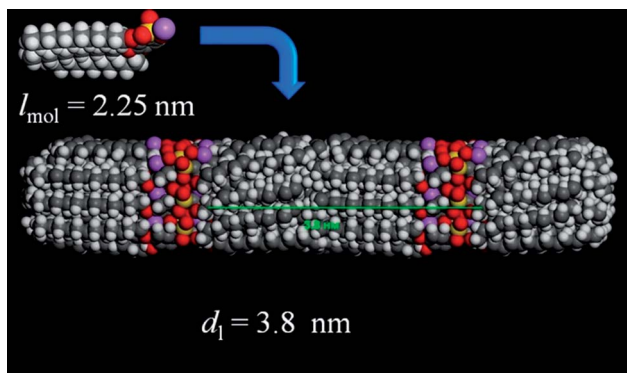


Fig. 3 Molecular modeling of a bilayer structure in lithium 2,3,4-tris(dodecyloxy)benzenesulfonate.

from a tapered slice, found in the smectic layers, to a conic one as present in the cubic mesophase. Reconstruction of electron density distribution revealed that the unit cell of the cubic mesophase contained eight different scatterers, two of them (type A) occupying special positions of the bcc lattice, while six others (type B) occupied special positions on cubic faces (Fig. 4).

It should be noted that these two types of scatterers have substantially different structures with different distributions of the electron density in their cores. The higher the temperature the less such difference is pronounced. Such an effect is followed by a merger of micelles in closest special position e (note an arrow in Fig. 4a) resulting in a phase transition to a primitive cubic lattice with unit cell parameter $a = 2.585 \text{ nm}$ (curves 4 and 5 in Fig. 2, corresponding data summarized in Tables S4 and S5 of ESI†). It is important to note that in the transition point, the primitive cubic lattice parameter is 0.56 of that in the $Pm\bar{3}n$ phase, the value being in very good agreement with the value of $5^{1/2}/4$ calculated from stereometric considerations. This transition is accompanied by a sharp increase of the average domain size, manifesting itself by a grain structure of reflections at temperatures higher than 170 °C.

Further heating of compound I leads to a decrease of the cubic lattice parameter down to $a = 2.56 \text{ nm}$ at 220 °C. The thermal expansion coefficient of the micellar primitive cubic phase was calculated to be $\beta = -1.5 \times 10^{-4} \text{ K}^{-1}$, which, by the order of value, is very common for liquid crystalline phases.^{31,32} For example, the high-temperature cubic mesophase of $Ia\bar{3}d$ symmetry formed by $(C_6F_{13}-C_2H_4O-C_6H_4-CH_2O)_3-C_6H_3-CO-(OCH_2CH_2)_4-OH$, *i.e.* gallic acid cores with long partially fluorinated alkyl tails, is characterized by an expansion coefficient of $\beta = -7 \times 10^{-4} \text{ K}^{-1}$.^{33–35} Such thermal behaviour of a material

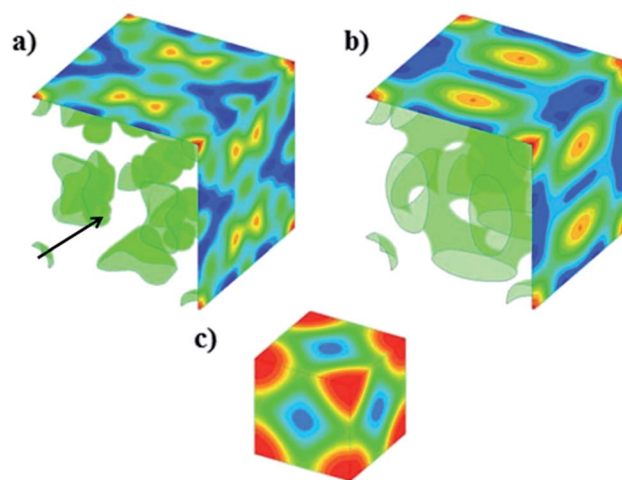


Fig. 4 Electron density maps of lithium 2,3,4-tris(dodecyloxy)benzenesulfonate at 100 °C (a), 130 °C (b) and 170 °C (c). Electron density distributions in the $Pm\bar{3}n$ phase were calculated using $-$, $+$ ($-$), $+$, $+$, $-$ ($+$) phase combination of reflections 200, 210 (120), 211, 422, 430 (340) leading to minimum values of the fourth moment of electron density fluctuations (3.89 and 2.44 at 100 °C and 130 °C respectively). On (100) planes, cross-sections of nodal surfaces are shown in (c), which were calculated using $+$, $+$, $-$, $-$, $-$, $-$ phase combination of 100, 110, 111, 200, 210, 222, 211 of a primitive cubic lattice ($\langle(\Delta\rho)^4\rangle = 2.13$).

can be explained by increasing concentrations of gauche-conformers in the alkyl tails of micellar periphery with increasing temperature. This in turn leads to a softening of the supramolecular aggregates, followed by their increased mobility and by corresponding compactization of the cubic mesophase. Cooling the samples of compound **I** down to room temperature resulted in the disappearance of the grain structure of cubic mesophase reflections, and to the redistribution of intensities of the reflections of $Pm\bar{3}n$ symmetry.

For instance, the 310 reflection completely disappeared at $T = 30^\circ\text{C}$. It should be emphasized that during all X-ray experiments, the studied samples were kept in a vacuum. At room temperature the cubic mesophase did not disappear over a period of several days of investigation, while annealing in the presence of air causes its collapse within one day. Diffraction patterns of such annealed samples contain only one broad reflection, which corresponds to an interlayer distance of $L = 3.45\text{ nm}$, indicating a partial recovery of the smectic order.

Thus, lithium 2,3,4-tris(dodecyloxy)benzenesulfonate is characterized by a bilayer crystalline structure of smectic type, which transforms to the micellar cubic mesophase of $Pm\bar{3}n$ symmetry at 130°C . The transition is probably driven by a change of the over-all shape of the mesogenic unit due to an effective decrease of the length of its aliphatic tails with increasing temperature. At 160°C , a more uniform distribution of alkyl-material between the micelles in different positions leads to the transformation to a primitive cubic mesophase.

Structure and phase behaviour of sodium 2,3,4-tris(dodecyloxy)benzenesulfonate

The sodium ion, compared to the lithium cation, has a larger diameter (1.02 \AA and 0.76 \AA respectively). In this section we shall explore how such a change of monodendrons' counter-ion size would affect the materials' phase behavior. DSC curves of sodium 2,3,4-tris(dodecyloxy)benzenesulfonate have much in common with thermograms of compound **I** (Fig. 5), though in the former case the transition peaks are found at lower

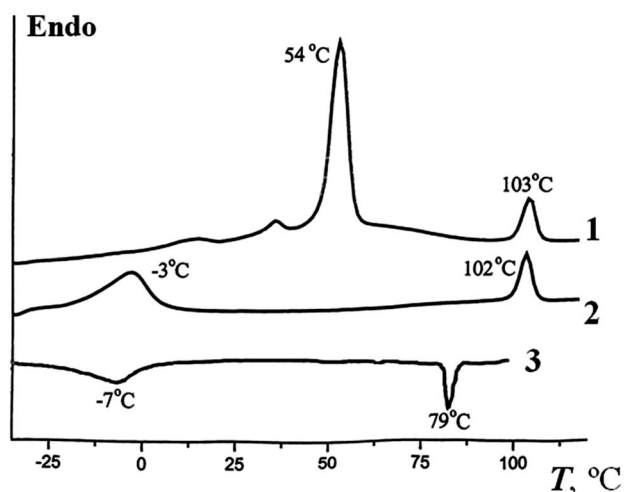


Fig. 5 DSC scans of sodium 2,3,4-tris(dodecyloxy)benzenesulfonate: (1) first heating, (2) second heating, and (3) first cooling.

temperatures. During the first heating run two peaks are observed at 54°C and 103.5°C (compare with 93°C and 118°C for compound **I**). Fusion heats are also lower for the sodium salt ($\Delta H_1 = 19.8\text{ kJ mol}^{-1}$; $\Delta H_2 = 3.7\text{ kJ mol}^{-1}$).

On cooling scans one can see two exothermic peaks at 80°C and -8°C with heats of fusion of 6.6 and 2.1 kJ mol^{-1} respectively. The substantial difference of the high-temperature peak position on heating and cooling scans can be explained by retarded kinetics of mesophase development at the heating/cooling rates used in experiments. Similar to lithium 2,3,4-tris(dodecyloxy)benzene sulfonate, the low-temperature peak of compound **II** can be ascribed to a crystal-mesophase transition.

Polarizing optical microscopy of as-received samples revealed the existence of crystalline domains up to 50°C . In support to these observations, SAXS patterns of sodium 2,3,4-tris(dodecyloxy)benzenesulfonate at room temperature (Fig. 6 and Table S6 of ESI†) contain 15 narrow reflections, which may be indexed by a cubic crystal lattice of $I\bar{2}3$ symmetry with lattice parameter $a = 6.18\text{ nm}$. Heating to 50°C is followed by its increase up to 6.24 nm ($\beta = 4.2 \times 10^{-4}\text{ K}^{-1}$).

Further heating leads to the development of a new set of reflections with d -spacing squares ratio $d_{10}^2 : d_{11}^2 : d_{20}^2 : d_{21}^2 = 1 : 3 : 4 : 7$ (Fig. 7 and Table S7 of ESI†), which is characteristic for a 2D hexagonal lattice. Wide-angle reflections disappear simultaneously at 50°C , unambiguously indicating the development of a disordered columnar mesophase. Its domains have an average size of 45.5 nm , being estimated by means of the Hoseman equation from the integral half-widths of 10 and 20 reflections, and its paracrystallinity parameter was equal to 3%. The cylinder diameter near the transition temperature was calculated to be 3.44 nm at 100°C , close to the observed interlayer distance in the smectic phase, formed by compound **I**. Thus, we can draw an important conclusion that in sodium 2,3,4-tris(dodecyloxy)benzenesulfonate the effective volume fraction of the mesogens' anionic groups is larger than that of compound **I**. So, the microphase segregation of the aromatic and aliphatic parts of benzenesulfonate molecules requires the

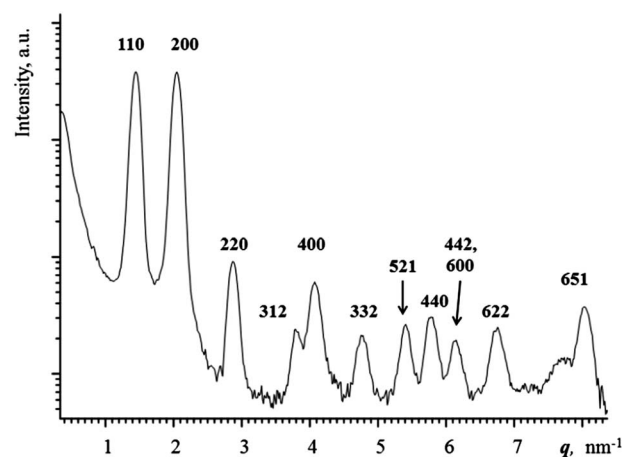


Fig. 6 Small-angle scattering diffractograms of sodium 2,3,4-tris(dodecyloxy)benzenesulfonate at room temperature. Indices of reflections of the cubic crystalline $I\bar{2}3$ phase are shown.

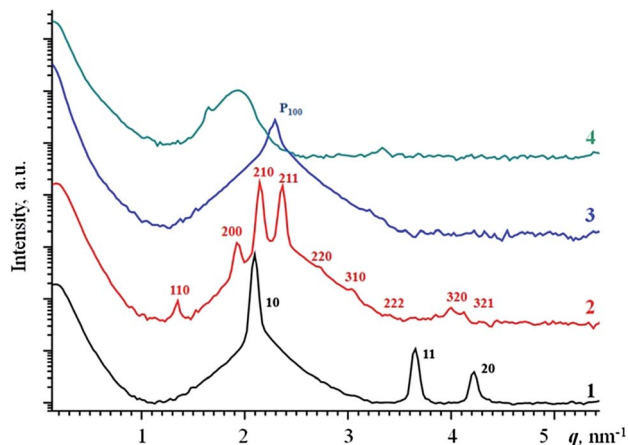


Fig. 7 Small-angle diffractograms of sodium 2,3,4-tris(dodecyloxy)benzenesulfonate at 100 °C (1), 140 °C (2), 240 °C (3) and at room temperature after cooling from 250 °C (4).

curvature of the interface between the ionic and electrically neutral micro-segregated phases to be of non-zero value at lower temperatures. This explains why in compound **I** a smectic phase is developed at low temperatures, while in compound **II** a columnar phase is formed. It should also be noted that the observed column diameter is smaller than double the length of sodium 2,3,4-tris(dodecyloxy)benzenesulfonate due to the reasons aforementioned.

The disordered columnar mesophase exists up to 118 °C. At 140 °C its high reflections disappear, and the first, strongest one shifts to the wider angle region ($d = 2.91$ nm), gaining simultaneously in half-width. With further heating, three reflections start to be resolved, the d -spacing squares ratio being equal to $d_{200}^2 : d_{210}^2 : d_{211}^2 = 4 : 5 : 6$, testifying to the development of the cubic mesophase of $Pm\bar{3}n$ symmetry ($a = 6.51$ nm at 140 °C; Fig. 7, curve 2, and Table S8 of ESI†). In compound **I**, the transition to the cubic mesophase of the same symmetry was observed ($a = 5.95$ nm) at the same temperature. The larger micellar size in compound **II** is due to the larger cations in the centres of the molecular aggregates. The temperature behaviour of the cubic phase of lithium- and of sodium benzenesulfonate salts is quite similar – in both materials a drastic growth of domain size has been observed at temperatures above 150 °C.

It is important to note the nature of the transition from columnar to cubic phase revealed by Fig. 8, which represents (111) projection of the electron density distribution in the $Pm\bar{3}n$ phase of compound **II** at 170 °C. One can see the remnants of late cylinders revealing the presence of a rotation axis of the sixth order in the cubic lattice.

Cooling compound **II** to 120 °C leads to the reversible transition into the disordered columnar mesophase, which is stable down to room temperature. Its column diameter changed to $D = 3.68$ nm, corresponding to a temperature expansion coefficient being equal to $-3 \times 10^{-4} \text{ K}^{-1}$. Negative values of temperature expansion coefficient in columnar mesophases have also been observed in compounds on the basis of gallic acid.^{36–38} This fact was explained by an extension of columns along their axis.

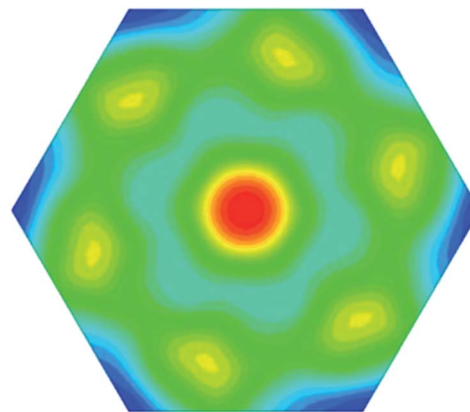


Fig. 8 (111) projection of electron density distribution in the cubic $Pm\bar{3}n$ phase of 2,3,4-tris(dodecyloxy)benzenesulfonate at 170 °C.

Annealing of sodium 2,3,4-tris(dodecyloxy)benzenesulfonate samples at room temperature in an air atmosphere leads to the substantial increase of column diameter up to $D = 3.77$ nm, possibly due to the relaxation of the aliphatic matrix.

Another explanation of this fact was mentioned when the temperature behaviour of lithium benzenesulfonate has been discussed, *i.e.* an impact of water molecules on the structure of supramolecular aggregates formed by benzenesulfonate mesogens. A detailed study of water absorption effects is a topic for a separate publication, which will follow later.

Further heating of the samples of compound **II** to the temperatures higher than 230 °C leads to the transformation of the $Pm\bar{3}n$ phase to the plastic crystal mesophase with a primitive cubic lattice (Fig. 7, curve 3), the effect is similar to that in compound **I**. However, the transition temperature is substantially higher for sodium 2,3,4-tris(dodecyloxy)benzenesulfonate (235 °C *vs.* 161 °C for the lithium salt). It should also be noted that a high-temperature primitive cubic mesophase is preserved until sample destruction – cooling the samples after 250 °C does not lead to the restoration of any ordered state due to the compound disintegration (Fig. 7, curve 4).

Structure and phase behaviour of potassium 2,3,4-tris(dodecyloxy)benzenesulfonate

The phase behavior of potassium 2,3,4-tris(dodecyloxy)benzenesulfonate (**III**) differs substantially from the temperature behaviour of the lithium and sodium benzenesulfonate salts. Thermograms of the first heating of compound **III** (Fig. 9) reveal four endothermic peaks at 18 °C ($\Delta H_1 = 22 \text{ kJ mol}^{-1}$), 47 °C ($\Delta H_2 = 5.8 \text{ kJ mol}^{-1}$), 123 °C ($\Delta H_3 = 4.6 \text{ kJ mol}^{-1}$), and 171 °C ($\Delta H_4 = 3.2 \text{ kJ mol}^{-1}$). Fusion heats of the last three of them are common for mesophase–mesophase transitions. However, polarizing optical microscopy reveals a fan-shape texture, which is characteristic for smectic and columnar mesophases, to be stable from room temperature up to 170 °C. Above this point samples of compound **III** are optically isotropic. This disappearance of the liquid crystalline texture is reversible.

Small-angle X-ray patterns of nascent potassium 2,3,4-tris(dodecyloxy)benzenesulfonate powder reveal more than

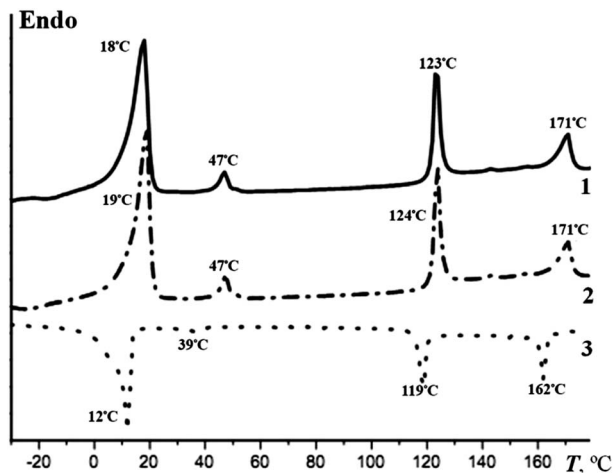


Fig. 9 DSC scans of potassium 2,3,4-tris(dodecyloxy)benzenesulfonate: (1) first heating, (2) second heating, and (3) first cooling.

twenty narrow reflections, indexed by a cubic crystal lattice of $I23$ symmetry with a lattice parameter $a = 6.39$ nm (Fig. 10 and Table S9 of ESI†).

Heating up to 50 °C is followed by the transition to a crystalline columnar mesophase with $a = 3.60$ nm and $c = 4.83$ nm ($P6/mmm$ symmetry), as is revealed by SAXS and WAXS patterns (Fig. 11 and Table S10 of ESI†). The average domain size, estimated with the use of Hosemann's equation, is 52 nm, the calculated paracrystallinity parameter equal to 2.9%. As it is common for supramolecular aggregates formed by alkali salts of asymmetric benzenesulfonate acid, the column diameter is substantially smaller than twice the length of the molecule (2.34 nm per molecule as is revealed by molecular modeling). This effect can either be explained by a tilt of the dendrons relative to the column axis (*pine-tree* structure) or by the interdigitation of aliphatic tails of dendrons belonging to neighbouring columns. Further heating up to 123 °C leads to the loss of wide-angle reflections, as well as of non-equatorial small-angle ones (Fig. 11, curve 2), indicating the development of the disordered

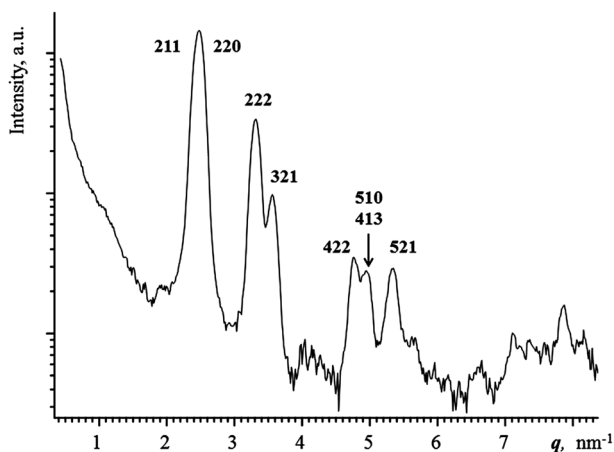


Fig. 10 Small-angle scattering of potassium 2,3,4-tris(dodecyloxy)benzenesulfonate at room temperature. Indices of reflections of the cubic crystalline $I23$ phase are shown.

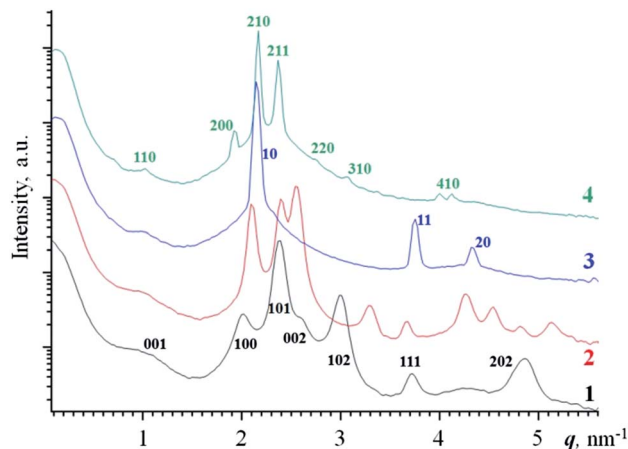


Fig. 11 Small-angle scattering for potassium 2,3,4-tris(dodecyloxy)benzenesulfonate at 100 °C (1), 120 °C (2), 170 °C (3) and 200 °C (4); two-digit indices show the reflections of the disordered columnar mesophase, three-digit ones correspond to the 3D hexagonal crystalline phase.

columnar phase. The transition includes the loss of crystalline order inside the columns, followed by the disappearance of intracolumnar register. The arrangement of the columns within the 2-D lattice, however, is retained (see ESI, Table S11†).

After cooling down to room temperature the intra-columnar order recovers, though with axial repeat $c = 4.84$ nm, compared with $c = 4.80$ nm at 50 °C on the transition to the columnar phase during the first heating.

Heating compound **III** up to 171 °C leads to the development of a cubic phase of $Pm\bar{3}n$ symmetry with the lattice parameter $a = 6.48$ nm (Fig. 11, curve 4, and Table S12 of ESI†) followed by a primitive cubic mesophase. The micellar size follows the trend of the other investigated alkali 2,3,4-tris(dodecyloxy)benzenesulfonates. With heating, the domain sizes become larger, as is manifested by the grain structure of small-angle reflections.

Cooling samples of compound **III** from the primitive cubic mesophase leads to the formation of a disordered columnar mesophase D_{hd} ($d = 3.37$ nm), which is stable down to the room temperature. On subsequent heating, a high-temperature transition to a cubic phase is observed, recognized from the increase of the relative intensity of 210 reflection due to the redistribution of electron density in the material. Thus, in compound **III**, compared with the other investigated materials, a low-temperature ordered columnar mesophase is observed. Moreover, the stability of the disordered columnar mesophase increases up to 171 °C (104 °C for sodium salt). However, the temperature behavior of potassium 2,3,4-tris(dodecyloxy)benzenesulfonate is quite complex: the “as-received” material forms a nascent crystal phase of $I23$ symmetry, which transforms at 50 °C to a crystalline columnar phase. At 123 °C the order inside columns is lost, and at 173 °C a cubic mesophase of $Pm\bar{3}n$ symmetry is developed.

Structure and phase behaviour of caesium 2,3,4-tris(dodecyloxy)benzenesulfonate

From the data shown above it is clear that gradual changes of the radius of the cation, which lies in the vicinity of the focal

point of the anionic part of the molecule, define changes of the effective mesogen shape, which, in turn, affects the phase behavior of the material. Caesium is the largest of alkali cations, whose salt has been studied in this paper. On the first heating scans of caesium 2,3,4-tris(dodecyloxy)benzenesulfonate (**IV**) one can see the only transition at 54 °C, having a substantial heat effect of 53 kJ mol⁻¹. It is not reproduced in subsequent heating-cooling scans. The second heating thermograms revealed two reversible transitions, one at 8 °C ($\Delta H = 9.3$ kJ mol⁻¹) and a second at 216 °C ($\Delta H = 3.4$ kJ mol⁻¹). At about 210 °C a *broken fan* texture also disappears, which is characteristic for optical micrographs of compound **IV** in a wide temperature range between the first and second transitions.

In “as-received” samples of caesium 2,3,4-tris(dodecyloxy)benzenesulfonate a cubic phase of *I23* symmetry with a lattice parameter $a = 6.69$ nm is observed. It should be remembered that at room temperature a cubic mesophase of the same symmetry has been observed in compounds **II** and **III** with the lattice parameters $a = 6.18$ nm and 6.39 nm respectively. Thus the structure of crystal-hydrates formed in “as-received” samples of alkali salts of 2,3,4-tris(dodecyloxy)benzenesulfonic acid is similar.

To verify this hypothesis we have carried out comparative analysis of the structure of the as-received sample of compound **IV** and of the same sample after a day in a vacuum. In the latter case small-angle reflections were significantly wider, high reflections have not been observed at all, pointing to the deterioration of crystal order due to the loss of hydrate crystals.

Heating up to 25 °C leads to the irreversible transition to the disordered columnar phase, characterized by four observed reflections with d -spacing square ratio $d_{10}^2 : d_{11}^2 : d_{20}^2 : d_{21}^2 = 1 : 3 : 4 : 7$ (Fig. 12).

Column diameters change linearly from 3.82 nm at 30 °C to 3.43 nm at 230 °C, the corresponding expansion coefficient being equal to $\beta = (-6.6 \pm 0.3) \times 10^{-4} \text{ K}^{-1}$. Crystalline domains grow simultaneously from 37.5 nm to 76.8 nm, while the paracrystalline parameter only weakly changed (3% at 30 °C and 3.5% at 230 °C).

The intensities of reflections of the disordered columnar phase did not change up to 230 °C. At this temperature a transition to the isotropic state has been observed. The first reflection of the columnar mesophase widened up to form an amorphous halo with a corresponding d -spacing of 2.87 nm.

Cooling the material down to room temperature leads to the development of complex scattering patterns, consisting of two sets of reflections, one of them corresponding to a column diameter of 4.2 nm, and the other one to a diameter of 3.82 nm. It is important that the relative intensities of reflections belonging to the different sets strongly depend on both temperature and the thermal history of the sample. The higher the temperature, the lower the intensity of the former set of reflections, and the stronger reflections of the latter set. At ~ 35 °C only one set of reflections remains. Such behavior of small-angle reflections is also in trend with the intensities of wide-angle reflections, which disappear at ~ 35 °C. To explain this behavior, one should investigate in detail DSC scans of the second heating run of compound **IV** (Fig. 13). The first

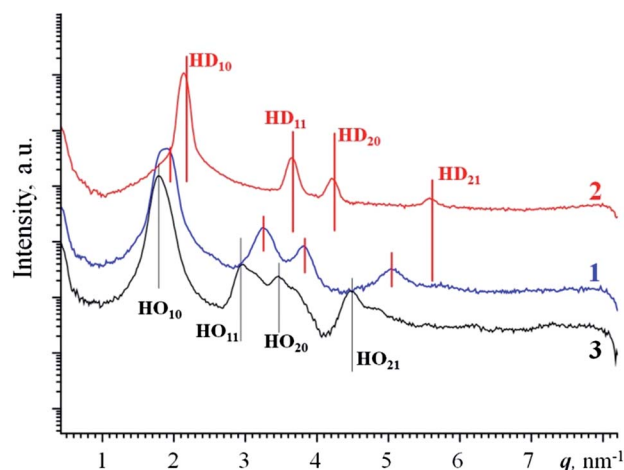


Fig. 12 Small-angle scattering for caesium 2,3,4-tris(dodecyloxy)benzenesulfonate at 50 °C (1), 230 °C (2), and 30 °C after cooling from 230 °C (3); reflections of ordered and disordered columnar mesophases (HO and HD respectively) are shown.

transition peak has a maximum at +8 °C; however the transition is rather broad and extends to 20–25 °C. Thus, it can be supposed that this DSC peak corresponds to an order–disorder transition inside the columns.

The detailed analysis of the structure of the columns in the ordered and disordered columnar mesophases, as well as the mechanism of transition between them will be the subject of a different paper in preparation now.

To conclude, in caesium 2,3,4-tris(dodecyloxy)benzenesulfonate at room temperature a mix of coexisting ordered and disordered columnar phases is observed. It should also be noted that in compound **IV**, unlike lithium, sodium and potassium salts of 2,3,4-tris(dodecyloxy)benzenesulfonic acid, a high-temperature cubic mesophase does not exist.

This is attributed to the substantial divergence of the shape of mesogen **IV** from the cone one. Therefore, development of spherical micelles becomes impossible, while columnar mesophases are stable up to isotropisation.

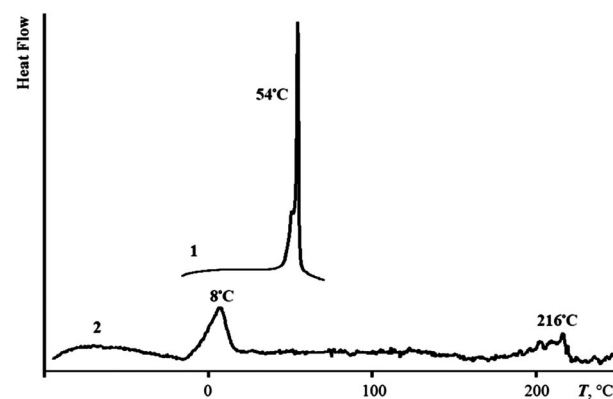


Fig. 13 DSC scans of caesium 2,3,4-tris(dodecyloxy)benzenesulfonate: (1) first heating and (2) second heating.

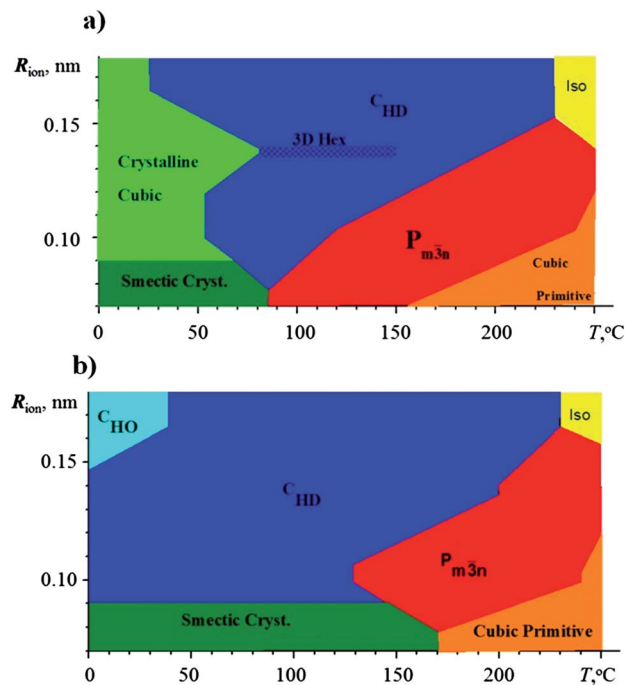


Fig. 14 Phase diagrams (cation radius R_{ion} vs. temperature) of alkali salts of 2,3,4-tris(dodecyloxy)benzenesulfonic acid as derived from the first (a) and following (b) heating cycles.

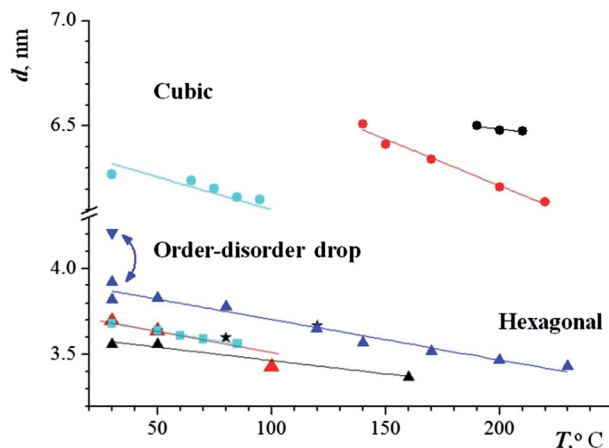


Fig. 15 Temperature dependencies of lattice parameters for alkali salts of 2,3,4-tris(dodecyloxy)benzenesulfonic acid: interlayer distance for smectic structures L (■); parameter a of the $Pm\bar{3}n$ cubic mesophase (●); column diameter D in crystalline (★), ordered (▼) and disordered columnar hexagonal mesophases (▲). Cyan markers stand for lithium salt, red – for sodium, black – for potassium and blue – for caesium.

Discussion and conclusions

Summarizing the discussion of the interrelation between the shape of the molecule, structure of supramolecular aggregates and phase behaviour of the material, one can make several important generalizations. Our investigation of the structure and phase behaviour of alkali 2,3,4-tris(dodecyloxy)benzenesulfonate revealed that variation of the volume ratio of the

organic anion to the inorganic cation leads to systematic changes in material temperature behaviour. The diameter of the cation varied in the range from ~ 0.102 nm to 0.167 nm, while the length of the aliphatic tails was the same in all four compounds studied. Mesophases of different types and dimensionalities were discovered: 1-D (smectic bilayers), 2-D (ordered and disordered columnar phases), and 3-D (crystalline hexagonal, high-temperature plastic crystals of $Pm\bar{3}n$ symmetry, low-temperature cubic phase of $I23$ symmetry). Below we carry out a comparative analysis of the structural and thermal characteristics of such mesophases, as well as of transitions between them. Phase sequences are represented in the phase diagram, associating the variation of the cation size with the temperature behaviour of the material as shown in Fig. 14. It should be emphasized that the phase behaviour of compounds I–IV on the first heating (Fig. 14a) is complicated by the formation of crystal hydrates and by their transformation due to the loss of water molecules. Thus, to establish an effect of the size of the focal group on the temperature behaviour of the material, we focus on the phase diagrams derived from the second heating scans (Fig. 14b) in our following considerations.

Several main conclusions can be drawn.

(1) Cubic types prevail, when the size of the cation is small, and the shape of the mesogenic group is close to a conic one. With increasing cation size, the shape becomes more tapered, and the columnar mesophase appears to be more stable.

(2) Increasing the cation size leads to a higher temperature of transition to the cubic plastic crystal mesophase. This fact can be explained by a variation of the free energy functional of self-assembled aggregates formed by different salts of benzenesulfonic acid. Obviously, an increasing dendron size leads to a stabilization of the columnar mesophase. Geometric aspects of this explanation can be found in ref. 18.

(3) The column diameters of the disordered columnar mesophases do not depend significantly on the size of the cation in alkali salts of 2,3,4-tris(dodecyloxy)benzenesulfonic acid.

(4) Ordered and disordered columnar phases can coexist in a rather wide temperature range, their lattice parameters (*i.e.* cylinder diameters) being substantially different. Moreover, intensity ratios of reflections are different as well, indicating that order-disorder transition inside columns is followed by (or caused by) the redistribution of electron densities.

It is also interesting to analyze the temperature dependencies of the lattice parameters in the studied compounds (Fig. 15). In any case at ambient temperature the cylinder diameter is in the range of 3.4–4.4 nm.

The loss of the order inside the columns does not lead to a considerable change of the thermal expansion coefficient β . However, the most pronounced feature of the D_{ho} to D_{hd} transition is a substantial (up to 10% with compound IV) jump down of the column diameter. This effect may be due to the shift of tapered dendrons to the centre of the cylinder, caused by an increased mobility of the dendrons and a corresponding loss of the order in the interior ion rim. Consequently, the most dramatic change is observed close to the column axis, where the low electron density of the ordered columnar mesophase switches to a high electron density in the disordered one.³⁵ Such

a change manifests itself in different ratios of the reflection intensities described above. The supramolecular cylinder can be regarded as a switchable ion channel, to be closed at higher temperatures and opened at lower ones.

In conclusion, the synthesized 2,3,4-tris(alkoxy)benzenesulfonates may be considered to belong to the class of "smart" thermotropic materials, exhibiting a rich variety of phase behavior, including phases of different symmetries and dimensionalities.

Notes and references

- U. Beginn, L. Yan, S. N. Chvalun, M. A. Shcherbina, A. V. Bakirov and M. Möller, *Liq. Cryst.*, 2008, **35**, 1073.
- U. Beginn, *Prog. Polym. Sci.*, 2003, **28**, 1049.
- V. Percec, C.-H. Ahn, T. K. Bera, G. Ungar and D. J. P. Yeardley, *Chem. – Eur. J.*, 1999, **16**, 1070.
- U. Beginn and G. Lattermann, *Mol. Cryst. Liq. Cryst.*, 1994, **241**, 215.
- G. Staufer, M. Schellhorn and G. Lattermann, *Liq. Cryst.*, 1995, **18**, 519.
- K. Borisch, C. Tschierske, P. Göring and S. Diele, *Chem. Commun.*, 1998, 2711.
- K. Borisch, S. Diele, P. Göring, H. Kresse and C. Tschierske, *J. Mater. Chem.*, 1998, **8**, 529.
- L. D. Landau and E. M. Lifshitz, *Statistical Physics*, (Fizmatlit, Moscow, 1995; Pergamon, Oxford, 1980), parts 1, 4.
- P. A. Smith, C. D. Nordquist, T. N. Jackson, *et al.*, *Appl. Phys. Lett.*, 2000, **77**, 1399.
- T. Thurn-Albrecht, J. DeRouchey, T. P. Russell and H. M. Jaeger, *Macromolecules*, 2000, **33**(9), 3250.
- X. L. Xu, S. A. Majetich and S. A. Asher, *J. Am. Chem. Soc.*, 2002, **124**(46), 13864.
- A. V. Bakirov, A. N. Yakunin, M. A. Shcherbina, S. N. Chvalun, X. Zhu, U. Beginn and M. Möller, *Nanotechnologies in Russia*, 2010, **5**(9–10), 41.
- X. Zhu, B. Tartsch, U. Beginn and M. Möller, *Chem. – Eur. J.*, 2004, **10**, 3871.
- V. Percec, M. Glodde, T. K. Bera, Y. Miura, I. Shiyonovskaya, K. D. Singer, V. S. K. Balagurusamy, P. A. Heiney, I. Schnell, A. Rapp, *et al.*, *Nature*, 2002, **419**, 384.
- J. N. Israelachvili, *Intermolecular and Surface Forces*, Acad. Press, New York, 1992.
- L. Leibler, *Macromolecules*, 1980, **13**, 1602.
- M. W. Matsen and F. S. Bates, *Macromolecules*, 1996, **29**, 1091.
- G. Ungar, Y. Liu, X. B. Zeng, *et al.*, *Science*, 2003, **299**, 1208.
- R. Hosemann and A. M. Hindeleh, *J. Macromol. Sci., Part B: Phys.*, 1995, **34**(4), 327.
- A. Guinier, *Theorie et Technique de la Radiocristallographie*, Dunod, Paris, 1956.
- V. S. K. Balagurusamy, G. Ungar, V. Percec and G. Johanson, *J. Am. Chem. Soc.*, 1997, **119**, 1539.
- P. Mariani, V. Luzzati and H. Delacroix, *J. Mol. Biol.*, 1988, **204**, 165.
- H. Sun, *J. Phys. Chem. B*, 1998, **102**, 7338.
- H. Sun, P. Ren and J. R. Fried, *Comput. Theor. Polym. Sci.*, 1998, **8**, 229.
- D. Rigby, H. Sun and B. E. Eichinger, *Polym. Int.*, 1998, **44**, 311.
- A. K. Rappé, C. J. Casewit, K. S. Colwell, W. A. Goddard and W. M. Skiff, *J. Am. Chem. Soc.*, 1992, **114**, 10024.
- C. J. Casewit, K. S. Colwell and A. K. Rappé, *J. Am. Chem. Soc.*, 1992, **114**, 10035.
- A. K. Rappé, K. S. Colwell and C. J. Casewit, *Inorg. Chem.*, 1993, **32**, 3438.
- M. W. Matsen and F. S. Bates, *Macromolecules*, 1996, **29**, 7641.
- L. Leibler, *Macromolecules*, 1980, **13**, 1602.
- E. Fontes, P. Heiney, M. Ohba, J. N. Haseltine and A. B. Smith, *Phys. Rev. A*, 1988, **37**, 1329.
- T. Sauer, *Macromolecules*, 1993, **26**, 2057.
- S. N. Chvalun, M. A. Shcherbina, I. V. Bykova, J. Blackwell and V. Percec, *Polym. Sci., Ser. A*, 2002, **45**, 1281.
- S. N. Chvalun, M. A. Shcherbina, A. N. Yakunin, J. Blackwell and V. Percec, *Polym. Sci., Ser. A*, 2007, **49**, 266.
- M. A. Shcherbina, A. V. Bakirov, A. N. Yakunin, V. Percec, U. Beginn, M. Möller and S. N. Chvalun, *Crystallogr. Rep.*, 2012, **57**(2), 151.
- S. N. Chvalun, J. Blackwell and Y.-K. Kwon, *Macromol. Symp.*, 1997, **118**, 663.
- S. N. Chvalun, J. Blackwell and J. D. Cho, *Polymer*, 1998, **39**(19), 4515.
- S. N. Chvalun, M. A. Shcherbina, I. V. Bykova, J. Blackwell, V. Percec, Y. K. Kwon and J.-D. Cho, *Polym. Sci., Ser. A*, 2001, **43**, 33.